Vol. 3, No. 1, pp. 88-116, (March 2022)
DOI: 10.21608/aujes.2022.69321.1016
Aswan University Journal of Environmental Studies (AUJES)
Online ISSN: 2735-4237, Print ISSN: 2735-4229
Journal homepage: https://aujes.journals.ekb.eg/ E-mail: AUJES@aswu.edu.eg
Original research

Primary dispersion patterns of gold and associated elements in Um Arka area, Allaqi Region, South Eastern Desert of Egypt.

Mohamed Abdallah Gad Darwish*[1], Herbert Poellmann[2], Doaa Abdel Gaber[1]

1. Geology department, Faculty of Science, Aswan University. Post No. 81528 Aswan, Egypt.
2. Department of Mineralogy and Geochemistry, Institute for Earth Sciences and Geography, Faculty of Science III, Martin-Luther University, Halle-Wittenberg, Germany

Received: 26/3/2021 Accepted: 19/1/2022

Abstract:

Um Arka area represents a portion of the Neoproterozoic Pan-African belt in the south Eastern Desert of Egypt. The present paper aims to investigate and evaluate the primary dispersion haloes of Au and associated elements. For this purpose, Au and associated elements have been determined in 105 quartz, dyke and country rock samples using both Inductively Coupled Plasma Optic Emission Spectrometry and Inductively Coupled Plasma Mass Spectrometry. Here, the statistical processing and mapping techniques of the analytical data have been applied. The results revealed that all the analyzed elements have been deviated from the normality, and there is a noticeable lack of correlation of both Au and Ag with As, Ba, Co, Cr, Cu, Fe, Ga, Hf, Hg, Mn, Mo, Nb, Ni, Pb, Rb, Sb, Sc, Sn, Sr, Th, Ti, U, V, Y, Zn, and Zr due to long history of Au mining activities. The primary dispersion patterns of Au, Ag, As, Hg and Sb referred to new sites of Au mineralization represented by the quartz veins, the country rocks, dykes, and tectonic zones. Moreover, Sn mineralization is expected to exist in the granitic rocks and Ni mineralization is expected to be in the metagabbroic rocks. Therefore, the area hosted three mineralized events involved Au-, Ni- and Sn- mineralizations that might be derived from a probable single major episode of mineralization sourced by hydrothermal solutions of Um Arka granitoid pluton. The primary dispersion patterns in the area were controlled by tectonic zones, lithology, and supergene processes. Finally, the Um Arka area is fruitful for Au-, Sn-, Ni-mineralization, and a promising target with success for the exploration project and starting new mining works.

Keywords: Primary dispersion patterns, Gold mineralization, Um Arka area, South Eastern Desert, Egypt.

1- Introduction

The geochemical patterns, which can be related to mineralization, are referred to as primary patterns or primary dispersion, irrespective of whether the reactions causing the element distribution patterns are syngenetic or epigenetic (James, 1967). Primary geochemical patterns in rocks were formed during different geological processes; they can be transmitted during weathering to various surficial materials (Xuejing and Binchuan, 1993).

Corresponding authors*: E-mail addresses: *mohamed.darwish26@yahoo.com*.

In fact, primary geochemical haloes and/or hypogene wall rock alterations are truly distinctive characteristics of the hydrothermal mineral deposits (Eilu and Mikucki, 1998; Govett and Atherden, 1988; McCuaig and Kerrich, 1998; Pirajno and Bagas, 2008; Safronov, 1936). Since the 1970s, geochemical pattern recognition techniques have been applied to recognize geological and the economic mineral resource information hidden in geochemical data (Briggs, 1978; Castillo-Munoz and Howarth, 1976; Collyer and Merriam, 1973; Gustavsson and Bjorklund, 1976; Howarth, 1973). Additionally, these techniques have been used to investigate the relations between regional geochemical patterns and large ore deposits (Xie et al., 2004).

In order to detect primary geochemical patterns, wall rock alteration, and related ore deposits, the lithogeochemical survey should be performed for reducing the risk and uncertainties of exploration, and costs of drilling too. Moreover, it helps to define the nature of primary dispersion patterns, elements associations, and pathfinder elements that are guide searches for buried ore deposits (Pantazis 1988).

Due to the continuously increasing gold prices in the global marketplaces at the end of the 1970s, the research proposals were fully funded all over the world for Au occurrences that were known from old surficial mining occurrences, simultaneously to geological and geochemical surveys (Varajão et al. 2000). Consequently, the gold exploration activities increased multifold in recent years and many exploration activities were focused in and around ancient gold mining districts, in both bedrocks and placer gold prospects.

In Egypt, more than 100 old and abandoned gold mines and occurrences are located in the Precambrian basement rocks of the Eastern Desert of Egypt (El Ramly et al. 1970; Sabet and Bordonosov 1984; Pohl 1988; Abdel Tawab 1992). In the south Eastern Desert of Egypt, especially in the Allaqi Region, there are more than eighteen ancient and abandoned gold mines. Most of these mines are spatially associated with Au bearing veins and veinlets hosted by shear zones, faults and fractures within the metasediments, ophiolitic mélange, island arc metavolcanics and related rocks, metagabbros, and dioritic and granitic rocks of Neoproterozoic age (El-Alfy 1986; Meneisy et al. 1986; Darwish 1996, 2004; El Shimi 1996; Tayae 2005). Among the previously mentioned Au locations, there is the deserted Um Arka Au mine which was chosen as the main object to perform this study.

During the past several decades, many studies have been performed in the study area for investigating different geological and geochemical aspects of regional geology and Au mineralization. These studies carried out by many authors (Kochin and Bassyouni, 1968; EGSMA 1996; El Shimi 1996; Noweir et al. 1996, 2001, 2007; El Fakharany 1997; Fawzy et al. 2000; Khalil et al. 2003; Khalil et al. 2014; Taye 2005; El Afandy 2007; Fawzy et al. 2012; Abdel Rahman et al. 2013; Klemm and Klemm 2013; El Dosouky et al. 2017, El-Desoky and El-Welaly 2018). Based on what was mentioned above, the present work aims to characterize and assess the primary geochemical patterns of the Au and associated elements that are considered as a tool for the exploration of hidden hydrothermal gold deposits, discover new sites of Au mineralization and related source, define the pathfinder elements and reach the exploration targets.

1.1. Um Arka area description

The Um Arka area is lying in the Allaqi region southernmost of the Eastern Desert located at a distance of about 217 Km south-east of Aswan city (Fig. 1a). Generally, the Um Arka area is defined by Lats. 22° 52\ N and 22° 59\ 30\\N and Longs. 33° 22\E and 33° 31\ E.

Historically, the gold in the Um Arka area was discovered and sporadically mined since the Pharaonic Era in the 19th and 20th Dynasties since 4000 B.C. (Hume 1937), Ptolemaic, Roman, Islamic periods, and until the twentieth century (1950s) as evidenced by conspicuous aspects of ancient mining activities. Klemm and Klemm (2013) monitored countless New Kingdom mills and runner stones scattered over the entire Um Arka area and antique ruins of the New Kingdom settlements. In addition to this, there is a well-preserved Arab settlement of Early Arab Period house complex, several tailings on the eastern side downstream of the Wadi Um Arka, and prayer sites in the Wadi center. Despite the fact that the gold of the Um Arka mine area was exploited from the surface and underground quartz veins and veinlets using numbers of shallow slit-like stopes, trenches, adits, and shafts, the exact amounts of Au production during these periods are not known. After 1956, the Au mine was closed due to the lack of required Au contents and processing facilities, governmental nationalization, and military considerations. Nowadays, the Um Arka area and surrounding environs are open for scientific research and investments. As a consequence, there is no significant industrialization, agricultural activities, and urban development throughout the study area.

1.2. Geology and Au-mineralization

The Um Arka area is considered as a lithological portion of the Arabian-Nubian Shield of the Neoproterozoic age (Stern 1994; Stein and Goldstein 1996). It, in turn, constitutes a part of the Pan-African Orogenic belt that forms a wide variety of Precambrian lithotectonic units exposed in the Eastern Desert of Egypt. The main rocks units exposed in the traversed area, as seen in Figure 1c, are as follows: (1) Ophiolitic metagabbroic rocks. (2) Late-tectonic granites represented by biotite granites. The mentioned granitoid intruded the preexisting rocks with intrusive sharp contacts. Finally, post-tectonic basic and acidic dykes, and quartz veins and veinlets invaded the formerly mentioned rock units.

Structurally, in spite of the whole Um Arka area was subjected to three phases of deformations, D1– D3 (Noweir et al. 1996), two shear zones cut the lithologic units of the traversed area; one is trending in WNW-ESE direction and another is possessing ENE-WSW direction. The latter has been hosted the main Au mineralization, in which digging and deepening of the ancient mine was performed.

The Au mineralization, the main mineralized quartz veins are generally trending ENE-WSW direction and steeply dipping toward NNW. They consist of several brecciated quartz lenses (10 m in length, 0.75m in width) connected by quartz veinlets constituting pinch and swell structures. They were located along with sheared contact between late tectonic granitoid and metagabroic plutons. Other mineralized quartz veins are located in the shear zone striking WNW-ESE and dipping 35-86^0 NNE, with maximum thickness equals to 75 cm and discontinuous length extending nearly 2400 m. The majority of the quartz veins have milky white and greyish white colour, while grey and smoky colours are less common. These veins are brecciated, sheared and fractured, and accompanied by the hydrothermal alteration with yellow to brown iron oxides at the footwall and clay minerals at the hanging wall. In general, the wall rock alterations of hydrothermal origin bounded the mineralized vein system in the Um Arka area are represented by pyritization, hematitization sericitization, carbonatization (El Shimi 1996). Mineralogically, the auriferous quartz veins and veinlets are mainly composed of: (a) gangue minerals represented mainly by quartz and minor amounts of carbonate (calcite or dolomite), and few sericite can be observed in some veins; (b) primary ore minerals included gold, pyrite, chalcopyrite, galena,

magnetite, covellite, pentlandite and millerite; and (c) supergene minerals consisted of hematite and goethite, limonite and malachite

2- Materials and Methods

2.1. Field sampling and sample treatments

In the field, a total of 105 surface samples have been collected from the country rocks exposed on both side of the shear zone hosted gold mineralization: 63 samples of metagabbroic rocks, 21 samples of granitic rocks, 10 samples of dykes, and 11 samples of quartz veins and veinlets. All samples were systematically gathered along 7 traverses that are running toward the NNE-SSW direction and perpendicular to the Au mineralized zone (WNW-ESE). The traverses cover an area of about 9.12 Km^2 with sample density equals 11.5 sample/ km^2 as seen in Fig. 1b. The distance between traverses equals to 250m, and the sample distance along each traverse is 200m with taking into account the lithology, topography, and mineralized zones. To minimize the sampling error at each sampling site, the composite sample of fresh material (weight 2-3kg) was collected from five sampling points over an area of nearly $25m^2$ using a geological hammer. In the laboratory, each composite sample was broken into small chips and crushed to chick-pea size using a geologic hand hammer and steel mortar, and then quartered to obtain the representative sample weighted nearly 250g. Subsequently, 100 g of each quartered and crushed sample was ground using a ball mill to obtain the fine homogeneous powder (-63μm) for the chemical analysis.

2.2. Sample leaching procedures and analytical measurement

For geochemical analysis, each powdered subsample was divided into 15 g using the cone and quarter method and oven-dried at < 40° C over one night. About 0.1 g of each ground subsample was treated with 2 ml HF (48%), 5 ml HNO_3 (65%), and 1 ml H_2O_2 (30%) in a closed Teflon vessel, and heated using the microwave. The digestion process was performed applying for the multiple stage programs; 6 min. at 1000W (160°C), 5 min. at 1000W (215°C), 19 min. at 700W (215°C) and finally, 20 min for ventilation. After cooling, all samples were heated and evaporated to remove HF, and then added 10mL of HNO_3. The obtained clear digested solutions were cooled to room temperature and diluted with de-ionized water in volumetric flasks to reach 50 ml for chemical analysis. Meanwhile, after filtration, the residual part of subsamples was treated with aqua regia (3 ml HNO_3 (65%) and 9 ml HCl (30%)) in a closed Teflon vessel using the same microwave. In this case, the digestion processes were done using another multiple-stage program; 10 min. (180°C), 10 min. (200°C), 20 min. (50°C), 10 min. (50°C) and 10 min. (50°C). Subsequently, the produced clear solutions were cooled to room temperature and diluted with de-ionized water in volumetric flasks to reach 50 ml for chemical analysis.

The generated solutions have been analyzed to determine a suite of chemical elements; Ag, As, Au, Ba, Co, Cr, Cu, Fe, Ga, Hf, Hg, Mn, Mo, Nb, Ni, Pb, Rb, Sb, Sc, Sn, Sr, Th, Ti, U, V, Y, Zn, and Zr, using both inductively coupled plasma optic Emission Spectrometry (ICP-OES) and inductively coupled plasma mass spectrometry (ICP-MS). All chemical analyses were carried out at Halle University Analytical Laboratories, Halle–Wittenberg, Germany. The quality control, accuracy, and analytical precision were performed using the calibration of both ICP-MS and ICP-OES instruments. As well as, analyses of certified standard reference materials (GBW 07112 Standard), blank samples, and replicate samples in each analytical set. Additionally, 10% of duplicate samples were re-analyzed, and the results of the blank solutions showed that all analyzed elements were below their corresponding lower detection limits. The 95% confidence interval is a measure of the certainty of the accuracy of the recommended value.

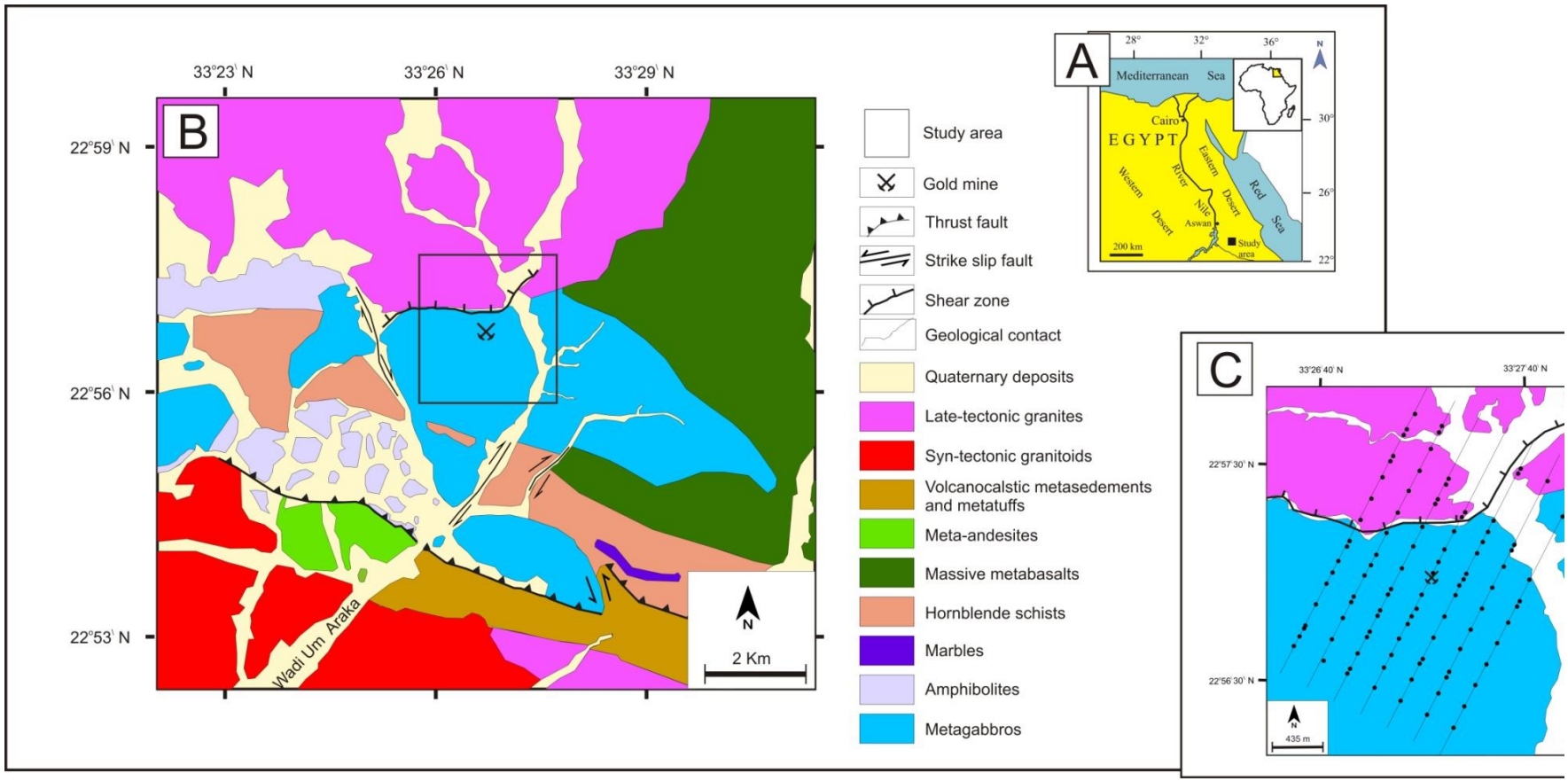

Fig. 1. Geological context of the Wadi Um Araka area, south-Eastern Desert of Egypt, (A) Sketch map showing location of the study area; (B) Geological map (modified after Noweir et al., 2007); (C) sampling stations represented by black circles.

2.3. Data processing

2.3.a. Statistical analysis

The statistical techniques used for this work are (1) basic descriptive statistics' methods (univariate statistics) are a benefit for identifying the overall features of the geochemical data and separating the background values and threshold of anomalies. Here the descriptive statistics include minimum, 25th, 50th, 75th, 90th, 95th, and 97th percentiles, maximum, mean, geometric mean, standard deviation, geometric standard deviation, variance, skewness, and kurtosis. Besides that, the Shapiro –Wilk test has been established for investigating the normality of raw and log-transformed geochemical data, applying the null hypothesis at a significance level of 0.05 (Table 1). The box and whisker plots of all analyzed chemical elements have graphically been drawn to show the variation of element concentrations in the rock samples of the study area. As well as, the geochemical data were tested by the Wilcoxon-signed rank test, applying the null hypothesis for comparing repeated measurements on a single sample to assess whether their population means or ranks differ. (2) Spearman's rank correlation coefficient (rs), (bivariate statistics), has been calculated to assess non-linear relationships and/or populations with a non-Gaussian distribution (Fowler et al., 1998) and the strength and direction (negative or positive) of a relationship between two elements in the geochemical data. (3) R-mode factor and cluster analyses (multivariate statistics) have been employed for re-interpreting and understanding of the geochemical patterns of arid desert terrains, giving helpful information for further exploration in similar terrains (Lin et al., 2014), evaluating the geochemical association of the analyzed elements and their potential sources. In this regards, factor analysis reduces the geochemical data into a set of new fewer factors, and the values of the factor matrix is improved by the Varimax rotation method to maximize the factor variance (Kaiser, 1958). On the other hand, R-mode cluster analysis classifies the analyzed elements into new groups (clusters), and discriminate various groups of trace elements as tracers of a natural source (Martínez et al., 2007). In this study, hierarchical cluster analysis produced by Ward's method and Euclidean distance is used to appreciate the close relationship among the factor scores generated by the R-mode factor analysis.

2.3.b. Geochemical maps production

The primary dispersion patterns of the Au and associated trace elements in the rock units can be manifested by constructing the isochemical maps because they are considered an important tool for qualitative and quantitative interpretation of these elements. Moreover, the geochemical maps are used to identify geochemical anomalies that are suggestive of mineralization (van Helvoort et al. 2005), provide important information to aid the search for mineral resources (Ohta et al. 2007), and be profitable for mineral exploration purposes (Ferguson and Kasamas 1999). The current investigation focuses on geochemical maps to yield invaluable information about the source, distribution, and dynamics of elements within the research area (Guillén et al. 2011). Here it is important to mention that geochemical maps are necessary to manifest the background value of Au and associated elements for delineating the sought anomalous parts that point out a new source or extension of Au mineralization in the area under investigation.

In the present study, geochemical maps were produced applying the box-plot method because it is a convenient way of graphical depicting groups of numerical data through their quartiles (Tukey 1997). Accordingly, the 50th percentile is accepted as background value since it possesses great robustness against extremes and outliers in the inhomogeneous and irregular geochemical data (Ohta et al. 2005; Jordan et al. 2007; Martínez et al. 2007); 95th percentile is considered as the

threshold value for anomaly definition (Williams et al. 2000; Wilde et al. 2004); and 97th percentile is a signal for the strong anomaly (Williams et al. 2000).

In this instant, the concentration levels of each element of interest are executed using six various colours that are indicative of six classes of its concentrations defined by the following intervals: minimum—25th percentile (yellow); 25th–50th percentile (green); 50th percentile—75th percentile (light blue); 75th percentile—95th percentile (blue); 95th percentile—97th percentile (dark blue); and > 97th percentile (red). The mentioned manner was useful and effective for drawing up the geochemical maps of the elements of interest for mineral exploration.

In addition to single element geochemical maps, factor scores generated by R-mode factor analysis have also been mapped for displaying the spatial distribution of multi-elemental associations and assess their spatial relationship with bedrocks and structure, and as well to establish a linear relationship (factor) among the associations.
The software employed in the present study for the statistical analyses and graphical presentation were Microsoft Excel 2010, OriginLab Version 18, and IBM SPSS Statistics Version 23. The geological map, and geochemical and factor score maps have been drawn using Arc GIS 10 (geographic information system), the CorelDraw graphic suite, Version 12, and Golden software Surfer, Version 16.

3. Results and Discussion

Geochemical data of the analyzed 28 variables (Ag, As, Au, Ba, Co, Cr, Cu, Fe, Ga, Hf, Hg, Mn, Mo, Nb, Ni, Pb, Rb, Sb, Sc, Sn, Sr, Th, Ti, U, V, Y, Zn, and Zr) existed in 105 bedrock, dyke and quartz vein samples have been statistically assessed using univariate, bivariate and multivariate analyses, graphical presentations and geochemical maps. The summary of the calculated statistical parameters obtained from geochemical data was listed in Table 1. It shows that Ag possesses concentration range (0.02 to 356.99 ppm) and mean value (5.41 ppm) greater than both the range value (0.01 to 15.58 ppm) and average value (0.22 ppm) of Au. The decrease in Au values might be due to the old traditional mining processes of Au in the past. Table 1 displays remarkable deviations between means and medians for the considered elements.

These deviations can be seen on the box and whisker plots represented by Figure 2 that presents the non-outlier range extended from upper and lower quartiles within 1.5 times the height of the box, the medians, mean values, and high outliers of all analyzed elements. It can be noted that all elements (except for Fe and Sr) have higher outliers without lower outliers and possess remarkable various degrees of displacement of mean values from median values toward either the 75th percentile or higher outliers. Clearly, the mean values of most analyzed elements such as Co, Cr, Fe, Ga, Hf, Hg Mn, Mo, Nb, Rb, Sc, Sr, U, V, Y, and Zn moved toward the limit of the 75th percentiles, whereas, the mean values of the other chemical elements exceeded their 75th percentiles and moved towards the high outliers.

Generally, it is known that the high outliers of Co, Cr, Mn, Ni, and Ti are indicative of mafic minerals in the metagabbroic rocks (Fairbridge, 1972), while the high outliers of Hf, Nb, Sn, Th, U, Y, and Zr are associated with heavy minerals existed in the granitic rocks. Additionally, the association of elements represented by Ag, As, Au, Hg, and Sb can be attributed to Au mineralization; meanwhile, Cu, Mo, Pb, and Zn might be referred to sulfides associated with Au mineralization (Jordan et al., 2007).

The measure of the asymmetry of the probability distribution “skewness” for the data distribution is deviated from zero value, illustrating that all analyzed elements are positively skewed (Table

1). Additionally, the measure of the tailedness of the probability distribution reveals that distributions of most elements are platy kurtic (kurtosis < 3), while a few elements like Fe, Sn, and Sr are described as leptokurtic (kurtosis > 3) as listed in Table 1.

Accordingly, the statistical distributions of all elements are deviated from the normality and considered as non-normal distribution. This finding is confirmed by Shapiro-Wilk (S–W) test, which illustrates that all the analyzed elements could not pass the normality test (p values < 0.05), rejecting the null hypothesis. For this reason, there is a real need to convert the natural geochemical data into logarithmic transformation (base 10) to improve their distribution toward normality.

Similarly, after log10-transformation of the present data, Shapiro-Wilk (S–W) test gave the same results for all elements (except for Cr and Th) showing no improvement toward the normality took place, and the null hypothesis adopted here is rejected too. Eventually, except for both Cr and Th, all analyzed elements are neither normally nor lognormally distributed, agreeing with Reimann and Filzmoser (2000) who mentioned that almost all geochemical data show neither a normal nor a lognormal data distribution, and when this fact is neglected, it will lead to biased or faulty results when parametric statistical methods are applied. Admittedly, this phenomenon exists in almost geochemical and environmental data (Reimann and Filzmoser 2000) due to a mixture of populations, outliers, analytical precision, and detection limits (Zhang et al. 2005). Under these circumstances, the log10 transformed data is preferable for calculating the multivariate statistical analysis to diminish the effect of outliers and extremes as possible, and avoid misleading and seriously biased results of both factor and cluster analysis.

Wilcoxon signed-rank test computation

The summary of the Wilcoxon signed-rank test computation exhibits the existence of statistically significant differences for the estimated median of Au against medians of all analyzed elements in natural and $\log_{10}$ transformed data (Table 2). As an illustration, they possess a two-tailed P-value less than 0.05, reflecting a rejection of the null hypothesis. In a like manner, except for the median value of $\log_{10}$ Hf (two-tailed p-value = 0.1856), the median value of Ag displays significant difference with medians of all elements in both normal and $\log_{10}$ transformed data. As a consequence of this, the null hypothesis is not agreeable too. No significant difference was found between the median of As and the medians of both Hf and Th (two-tailed p-value = 0.3845 and 0.59125, respectively) in the raw data, indicating an acceptance of the null hypothesis and a rejection of the remaining elements. In $\log_{10}$-transformed data, the median of As displays a significant difference with those of all analyzed elements, suggesting that the null hypothesis is unacceptable. Regarding the median of Hg against medians of all concerned elements, they exhibit significant differences, at p-values < 0.05, in both natural and $\log_{10}$-transformed data, and then their medians without exception could not succeed to pass the Wilcoxon signed-rank test. Despite the median of Sb exhibits a statistically significant difference with all analyzed elements ($p< 0.05$), it does not show this difference with the medians of both Hf and Th ($\log_{10}$-transformed data) as shown in Table 2.

Therefore, in this case, the medians of $\log_{10}$ data of both Hf and Th could pass the Wilcoxon signed-rank test while those of the other elements fail to override it.

Table 1. Summarized statistics and the average concentrations in the upper continental crust of the earth of the chemical elements distributed in the rock sampling stations (N=105).

Element	Unit	Minimum	25th percentile	50th percentile	75th percentile	90th percentile	95th percentile	97th percentile	Maximum	Mean	Geometric Mean	Standard Deviation	Geometric Standard Deviation	Variance	Skewness	Kurtosis	Shapiro-Wilk Test		UCC
																	p-value raw data	p-value Log data	
Ag	ppm	0.02	0.06	0.10	0.30	0.74	1.43	3.41	356.99	5.41	0.15	38.90	4.60	1513.28	8.14	69.16	0.000	0.000	0.05
As	ppm	0.08	0.08	0.28	0.70	1.77	1.94	2.38	34.47	0.92	0.28	3.51	3.58	12.30	8.80	82.87	0.000	0.000	1.50
Au	ppm	0.01	0.02	0.04	0.08	0.19	0.35	0.37	15.58	0.22	0.04	1.52	3.79	2.31	10.11	103.02	0.000	0.000	0.002
Ba	ppm	2.35	47.32	70.20	154.75	310.92	552.0	768.2	99488.4	1362.74	83.39	10109.9	4.16	102209000	9.19	88.00	0.000	0.000	550
Co	ppm	0.18	1.16	8.00	16.06	27.40	32.25	46.27	73.00	11.19	4.86	12.54	4.79	157.16	2.09	6.07	0.000	0.000	10.0
Cr	ppm	15.14	67.43	115.10	190.32	334.07	474.19	548.23	1612.81	169.34	118.02	189.96	2.32	36083.9	4.69	31.87	0.000	0.839	35.0
Cu	ppm	2.07	8.90	14.21	22.48	41.83	59.85	90.44	489.17	24.62	14.89	50.24	2.37	2524.1	7.93	71.81	0.000	0.012	25.0
Fe	ppm	1331.1	8840	20571.1	31761.9	49774	56846.6	56884.5	59707.3	22965.4	17077.4	15757.9	2.38	248313000	0.75	-0.32	0.000	0.001	35000
Ga	ppm	0.17	4.44	7.57	10.55	12.98	16.20	19.70	94.64	9.21	6.05	12.69	2.75	161.14	5.91	38.38	0.000	0.000	17.0
Hf	ppm	0.00	0.03	0.12	0.72	2.01	3.07	3.42	7.33	0.70	0.12	1.31	10.82	1.72	3.24	12.08	0.000	0.000	5.80
Hg*	ppm	0.01	0.01	0.04	0.07	0.14	0.18	0.20	0.56	0.06	0.03	0.07	3.16	0.01	3.59	19.85	0.000	0.000	0.05
Mn	ppm	16.50	186.43	258.8	388.10	668.37	907.44	993.47	3618.28	352.90	241.47	403.86	2.51	163104	5.46	41.22	0.000	0.000	600
Mo	ppm	0.10	0.28	0.40	0.61	1.14	1.69	2.05	5.88	0.62	0.44	0.79	2.09	0.62	4.58	25.18	0.000	0.001	1.50
Nb	ppm	0.01	0.34	1.12	6.46	14.99	21.84	33.79	39.33	5.15	1.26	8.31	7.34	69.08	2.39	5.73	0.000	0.005	25.0
Ni	ppm	1.01	3.01	25.29	70.49	130.34	313.50	337.90	1138.3	73.47	19.16	168.16	5.56	28277.8	5.08	29.33	0.000	0.000	20.0
Pb	ppm	0.34	1.17	1.86	6.25	12.06	15.28	21.50	895.03	13.32	2.67	87.21	3.37	7606.0	10.13	103.33	0.000	0.000	20.0
Rb	ppm	0.16	1.84	4.48	15.97	22.75	30.58	34.54	86.47	9.25	4.08	11.96	4.27	143.00	3.11	15.88	0.000	0.004	112
Sb	ppm	0.03	0.11	0.17	0.31	0.56	0.92	1.01	11.28	0.36	0.20	1.10	2.30	1.22	9.53	94.80	0.000	0.000	0.20
Sc	ppm	0.13	0.71	2.58	6.73	11.00	12.93	15.91	55.18	4.72	2.01	6.69	4.51	44.75	4.56	30.87	0.000	0.000	11.0
Sn	ppm	0.41	0.97	1.43	5.10	58.60	74.12	80.18	94.52	12.88	2.96	24.43	4.78	596.67	2.06	2.89	0.000	0.000	5.50
Sr	ppm	12.61	37.03	141.26	245.6	308.86	341.79	361.21	378.43	149.29	96.94	113.50	2.85	12881.3	0.36	-1.21	0.000	0.000	350
Th	ppm	0.00	0.04	0.13	0.70	2.50	6.69	7.33	16.73	1.11	0.16	2.69	7.99	7.21	4.08	18.94	0.000	0.167	10.7
Ti	ppm	13.52	728.2	1328.3	3117.0	9713.4	12036.7	17349.5	38060.6	3445.0	1357.6	5558.8	4.74	30900000	3.75	18.61	0.000	0.002	3000
U	ppm	0.10	0.29	0.36	0.94	1.64	1.91	2.50	3.77	0.70	0.49	0.70	2.25	0.49	2.25	5.89	0.000	0.000	2.80
V	ppm	0.04	0.04	10.59	37.63	76.85	98.99	149.30	357.41	29.76	3.30	50.74	21.77	2574.7	3.94	21.25	0.000	0.000	60.0
Y	ppm	0.07	0.39	1.30	4.12	17.26	21.19	22.34	33.08	4.22	1.31	6.74	5.18	45.42	2.22	4.35	0.000	0.011	22.0
Zn	ppm	5.83	13.75	21.43	44.83	61.41	86.15	92.63	935.35	42.24	24.92	100.7	2.25	10144.1	7.66	63.70	0.000	0.000	71.0
Zr	ppm	0.15	0.91	2.57	15.78	59.34	98.89	111.64	278.18	20.46	4.09	44.10	6.46	1945.1	4.01	19.02	0.000	0.004	190

UCC: average concentration of the chemical elements in the upper continental crust of the earth (after Taylor and McLennan, 1995, while Hg after Beus and Grigorian 1977).

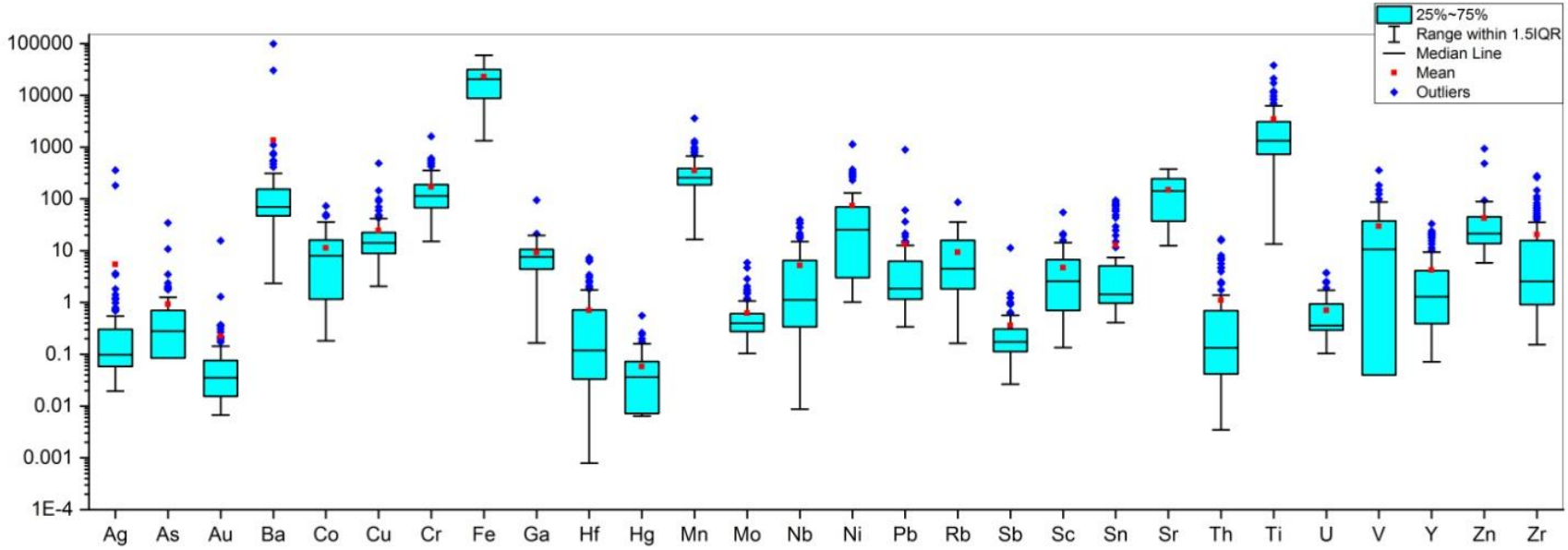

Fig. 2. Box and whisker plots of the chemical elements distributed in the studied rock sampling stations (N=105).

Table 2. Results of Wilcoxon signed-rank test for the chemical elements versus As, Ag, Au, Hg and Sb distributed in the rock sampling stations (N=105).

	Ag		As		Au		Hg		Sb	
	p-raw	p-log	p-raw	p-log	p-raw	p-log	p-raw	p-log	p-raw	p-log
Ba	0.0000	0.0000	0.0000	0.0000	0.0000	0.0000	0.0000	0.0000	0.0000	0.0000
Co	0.0000	0.0000	0.0000	0.0000	0.0000	0.0000	0.0000	0.0000	0.0000	0.0000
Cr	0.0000	0.0000	0.0000	0.0000	0.0000	0.0000	0.0000	0.0000	0.0000	0.0000
Cu	0.0000	0.0000	0.0000	0.0000	0.0000	0.0000	0.0000	0.0000	0.0000	0.0000
Fe	0.0000	0.0000	0.0000	0.0000	0.0000	0.0000	0.0000	0.0000	0.0000	0.0000
Ga	0.0000	0.0000	0.0000	0.0000	0.0000	0.0000	0.0000	0.0000	0.0000	0.0000
Hf	0.0007	**0.1856**	**0.3845**	0.0016	0.0000	0.0000	0.0000	0.0000	0.0121	**0.3656**
Mn	0.0000	0.0000	0.0000	0.0000	0.0000	0.0000	0.0000	0.0000	0.0000	0.0000
Mo	0.0000	0.0000	0.0000	0.0000	0.0000	0.0000	0.0000	0.0000	0.0000	0.0000
Nb	0.0000	0.0000	0.0000	0.0000	0.0000	0.0000	0.0000	0.0000	0.0000	0.0000
Ni	0.0000	0.0000	0.0000	0.0000	0.0000	0.0000	0.0000	0.0000	0.0000	0.0000
Pb	0.0000	0.0000	0.0000	0.0000	0.0000	0.0000	0.0000	0.0000	0.0000	0.0000
Rb	0.0000	0.0000	0.0000	0.0000	0.0000	0.0000	0.0000	0.0000	0.0000	0.0000
Sc	0.0000	0.0000	0.0000	0.0000	0.0000	0.0000	0.0000	0.0000	0.0000	0.0000
Sn	0.0000	0.0000	0.0000	0.0000	0.0000	0.0000	0.0000	0.0000	0.0000	0.0000
Sr	0.0000	0.0000	0.0000	0.0000	0.0000	0.0000	0.0000	0.0000	0.0000	0.0000
Th	0.0001	0.0236	**0.5912**	0.0107	0.0000	0.0000	0.0000	0.0000	0.0232	**0.6942**
Ti	0.0000	0.0000	0.0000	0.0000	0.0000	0.0000	0.0000	0.0000	0.0000	0.0000
U	0.0000	0.0000	0.0000	0.0000	0.0000	0.0000	0.0000	0.0000	0.0000	0.0000
V	0.0000	0.0000	0.0000	0.0000	0.0000	0.0000	0.0000	0.0000	0.0000	0.0000
Y	0.0000	0.0000	0.0000	0.0000	0.0000	0.0000	0.0000	0.0000	0.0000	0.0000
Zn	0.0000	0.0000	0.0000	0.0000	0.0000	0.0000	0.0000	0.0000	0.0000	0.0000
Zr	0.0000	0.0000	0.0000	0.0000	0.0000	0.0000	0.0000	0.0000	0.0000	0.0000

Bold values are greater than 0.05, The values below 0.001 are replaced by 0.0000

As shown above, it can be concluded that As, Ag, and Sb are most expected to be associated with the emplacement of granitic plutons due to their close relation with Hf and Th because the latter two elements can accommodate in the structures of zircon and monazite that co-existed in these plutons.

Normalization UCC

In order to define the variation and relationship between the interesting elements, eliminate redundant (useless) data, and increase the clarity in organizing data, the normalization has been computed. Here the normalization is justified because it is regarded as a convenient reference for comparing the analyzed elements derived from the country rocks with their related source in the study area. In this respect, the mean and median values of each element have been normalized to their corresponding average concentrations in the upper continental crust of the earth (Taylor and McLennan, 1995, and Beus and Grigorian 1977) as listed in Table 3.

This table shows that the normalized mean values of Au (903.54), Ag (23.39), Hg (2.11), and Sb (1.6) in quartz veins are higher than their corresponding average contents in the upper continental crust of the earth. Besides quartz veins, remarkable high normalized values of Au (37.86) and Ag (716.21) in dyke; Au (29.4), Ag (1.83), As (1.54), and Sb (1.49) in granitic samples; and Au (33.43), Ag (62.03), Hg (1.43) and Sb (2.08) in the metagabbroic rocks have been recorded if compared with their average content in the upper continental crust (Table 3).

Regarding the normalized results of Ag, Hg, and Sb, they lead to proposing that these elements are closely associated with Au mineralization that existed in the area; hence, they are considered as indicative of the Au mineralization. Overall, it can be concluded the aforementioned dyke and country rocks exposed in the Um Arka area are expected to have Au mineralization in addition to the mineralized quartz veins.

dyke (2.1), granites (4.94), and metagabbros (4.8) are possible due to a presence of Cr as common impurities in the structure of magnetite and calcite existed in quartz veins and the country rocks. Moreover, Cr can also host in the structures of chlorite, biotite, rutile, and pyroxene of the mentioned country rocks and dykes. The increasing of the normalized average value of Ni (5.49) in the metagabbroic samples and of Sn (6.93) in granitic samples is a signal of the presence of Ni sulphides and Sn-bearing minerals, respectively, in the mentioned rocks. On the contrary, the decreasing of the normalized mean and median values (< 1) of remaining elements is probably a result of their mobility and depletion under supergene processes.

Spearman-Rank correlation coefficient

The matrix of the Spearman– Rank correlation coefficient (Table 4) shows strong positive correlations of Fe with V, Mn, Ni, and Sc, exhibiting rs values equal 0.63 (Fe–V), 0.64 (Fe –Mn), 0.72 (Fe –Ni) and 0.74 (Fe –Sc). Similarly, Sc exhibits strong positive correlations with Ti, Y and V (rs= 0.61, 0.69 and 0.75, respectively). Also, Table 4 presents that Ni is positively correlated with Fe (rs=0.72) and Sr (rs=0.66), and very strongly correlated with Co (rs=0.91). Likewise, V shows a very strong positive correlation with Ti (rs=0.97). As a consequence of the stated correlations, they refer to the ferromagnesian minerals in mafic rocks, whilst the very strong correlation between Co and Ni (rs=0.91) is due to that fact that Co is considered as common impurities in pentlandite $(Fe, Ni)_9S_8$) and millerite (NiS) that are scattered in the mafic rock. This finding is supported by the high normalized mean value of Ni (5.49) as seen in Table 3. Conversely, there is no correlation between Cr and Ni (0.00) this reflects that Cr ion could not accommodate in crystal lattices of Ni-sulfides; whereas, it could host in the structures of some

oxides (e.g., magnetite) and silicate minerals (such as pyroxene and amphibole) that are existed in the metagabbroic rocks.

Table 3. Results of the normalized mean and median values, relative to UCC, of the chemical elements distributed in the rock sampling stations (N=105).

Element	Quartz veins		Granitic rocks		Dykes		Metagabbroic rocks	
	Mean/UCC	Median/UCC	Mean/UCC	Median/UCC	Mean/UCC	Median/UCC	Mean/UCC	Median/UCC
Ag	23.39	14.83	1.83	1.51	716.25	1.00	62.03	2.10
As	0.96	0.06	1.54	0.46	0.21	0.06	0.31	0.08
Au	903.54	47.32	29.40	21.19	37.86	12.96	33.43	16.71
Ba	0.26	0.10	0.14	0.12	0.25	0.14	4.00	0.15
Co	0.18	0.08	0.46	0.06	0.99	0.91	1.52	1.16
Cr	7.35	8.67	4.94	4.56	2.10	1.74	4.80	3.24
Cu	0.60	0.54	0.30	0.24	0.91	0.73	1.29	0.69
Fe	0.27	0.23	0.28	0.22	1.12	1.23	0.79	0.67
Ga	0.20	0.14	0.80	0.58	0.81	0.26	0.47	0.46
Hf	0.16	0.04	0.36	0.30	0.13	0.11	0.03	0.01
Hg*	2.11	1.79	0.47	0.28	0.85	0.43	1.43	1.05
Mn	0.26	0.23	0.46	0.38	0.85	0.65	0.65	0.45
Mo	0.93	0.40	0.27	0.24	0.39	0.28	0.38	0.27
Nb	0.27	0.15	0.52	0.38	0.21	0.09	0.09	0.02
Ni	0.33	0.20	1.03	0.12	1.46	0.91	5.49	2.13
Pb	0.25	0.12	0.47	0.43	0.11	0.07	0.89	0.08
Rb	0.15	0.12	0.13	0.14	0.06	0.04	0.06	0.02
Sb	1.61	0.91	1.49	1.05	0.92	0.65	2.08	0.84
Sc	0.67	0.22	0.04	0.02	0.84	0.91	0.45	0.37
Sn	0.41	0.29	6.93	5.36	0.38	0.28	0.99	0.19
Sr	0.15	0.13	0.10	0.06	0.31	0.21	0.60	0.63
Th	0.23	0.08	0.07	0.03	0.22	0.08	0.08	0.01
Ti	0.19	0.10	0.47	0.40	2.73	3.27	1.31	0.64
U	0.31	0.18	0.50	0.45	0.18	0.17	0.17	0.11
V	0.06	0.00	0.19	0.00	1.58	1.26	0.49	0.33
Y	0.37	0.14	0.06	0.01	0.42	0.35	0.17	0.07
Zn	0.32	0.19	0.93	0.70	0.71	0.66	0.51	0.29
Zr	0.07	0.03	0.38	0.26	0.07	0.05	0.03	0.01

UCC: average concentration of the chemical elements in the upper continental crust of the earth (after Taylor andMcLennan, 1995, while Hg after Beus and Grigorian 1977).

On the other hands, the enhancement of normalized mean values of Cr in the quartz veins (7.35), On the other hand, there are the strong positive correlations (0.600 > rs < 0.800) of U with both Zr and Rb; Th with Zr, Y, and U; Zr with Rb, Pb, and Nb; Hf with both U and Sn; Nb with U, Pb, and Rb; and the latter with both Th and Hf. At the same time, the correlations between Hf and both Zr and Nb are very strong (0.800 > rs < 1.000). Consequently, these correlations are suggestive of the close affinity of these elements with zircon, monazite, and xenotime that are

associated with granitic rocks. For instance, Y, Nb, Hf, Th, and U are related to zircon (Kitajima et al. 2012), which has a capacity to host these elements into its structure by simple or coupled substitutions (Hoskin and Schaltegger 2003; Fu et al. 2008; Bouvier et al. 2012). As well as, Y, Th, and U are coexisted in the crystal lattice of monazite (Bea 1996; Jiao et al. 2013) and xenotime (Broom-Fendley et al. 2016). As regards the strong correlations of Sn with Zr, Hf, and Nb, they are referring to a significant signal for the existence of disseminated cassiterite in the granitic pluton because the normalized value of Sn reaches 6.93 in granitic samples (Table 3).

A noticeable lack of correlation of Au with other chemical elements might be due to either the disturbances caused by the long history of Au mining activities in the past as it was previously stated or Au was concentrated at the preferred depth. In like manner, the correlations between Ag and all analyzed elements (except Hg) are below any significant value because Ag is soluble under oxidizing conditions at lower temperatures and moderate to low pH (Maynard, 1983). Afterward, Ag might probably be transported to alluvium deposits to concentrate at a preferable depth of 10-20 cm (Reedman, 1979) or moved downward within the fracture system of county rocks to concentrate on deeper levels.

Geochemical maps

Isochemical maps for Au and the associated elements, such as Ag, As, Hg, and Sb, at the Um Arka area have been constructed due to their known significance for exploring the Au mineralization (Figs. 3 and 4).

Also, take into account the considered maps are important to delineate a new fruitful anomalous site, which is likely referring to a new source or an extension of Au-mineralization in the investigated area. By the same token, both Ni and Sn have been chosen to draw up the geochemical map because both elements have high normalized mean values as previously stated (Table 3). The present study reveals the strong anomaly of Au does not appear in all sites throughout the Um Arka area, but it is restricted to the location of the ancient Au mine (Fig. 3). Another expectable explanation is suggesting that the Au content might be increased at deeper levels along the structure system affecting the area. The generated Ag anomalous patterns are associated with both Au and As anomalies at the location of the abandoned Au mine and recorded in the granitic pluton also (Fig. 3).

With increasing the Ag content, the considerable strong anomalous patterns of Ag have been observed at the southwestern and eastern parts of the traversed area. This maybe reflects that these anomalies are tectonically controlled by the shear zones and the buried structure in the traversed area. Accordingly, the strong dispersion haloes of Ag are the most important and require further investigations. Likewise, two strong As anomalies are recorded in the area: one anomalous pattern has existed along the ancient Au mine associated with the Au anomaly, and another anomaly is located at the southwest of the Au mines (Fig. 3). Both anomalies of As are structurally controlled and trended NW-SE direction, which is concordant with the shear zone of the area. Similarly, Figure 4 shows three strong anomalies of Hg possessing the same direction (NW-SE): the first anomaly is small and located at the deserted Au mine in accordance with anomalies of Au, Ag, and As; the second anomaly is situated at the southeast of the mine; the third anomaly is significant and occupies the southwestern corner of the traversed area in accordance with the strong anomaly of Ag. As can be seen from Figure 4, two small strong anomalous patterns of Sb coincide with primary patterns of Ag, As, Au, and Hg, suggesting a considerable harmonization due to the fact that they are predominantly observed at the mentioned Au mine location. As well as, the southeastern corner of the traversed area is covered by a big

pattern of strong Sb anomaly. Accordingly, it can be concluded that Ag, As, Hg, and Sb are effective for defining a new source of Au in the area and significant for performing the geochemical exploration, taking into account that these elements can be advised as the pathfinders for carrying out the exploration project of Au in the area and its environs. As shown in Figure 3, a strong anomalous pattern of Cr is sub-parallel to the Ni anomalous pattern at the southwest of the mine. This is due to a lack of correlation between both elements, and, moreover, Cr is not a common impurity in Ni sulfides.

Despite geochemical patterns of strong anomalous patterns of Ni are clearly distributed in the metagabbroic rocks and aligned parallel to the shear zone, they are not concordant with those of Ag, As, Au, Hg, and Sb (Figs 3 and 4). In the same manner, Figure 4 displays that the dispersion pattern of strong anomalous of Sn is commonly restricted to the granitic pluton. Accordingly, geochemical patterns of both Ni and Sn reflect a strong possibility of the existence of Ni-mineralization in the metagabbroic rocks and Sn mineralization in granitic rocks.

In a light of an existing three mineralization types, it can be suggested they are likely representing three separated mineralized events in the primary environments and forming an expectable single major episode of mineralization sourced by magmatic-hydrothermal solutions that derived from the granitoid pluton in the research area.

In general, the distribution of dispersion haloes of Au, Ni, and Sn in the primary environment of the Um Arka area is not randomly distributed, but they were controlled by the feeding channels represented by the shear zones, faults, and hidden fracture system. Furthermore, lithology could play an important role to feed and control the localization of the mentioned mineralizations.

R-mode Factor analysis

The geochemical data have been reduced to 10 synthetic factors based on eigenvalue greater than one, accounting for 68.1% of the total variance (Table 5). Also, the produced communalities and factor loadings have been shown in Table 6. The first four factors with geochemical similarities, defining four geochemical associations were interpreted because the other elements tend to possess either very low communalities or a tendency to form independent factors. Hence the considered four factors are as follows:

Factor 1 accounts for 10.27 of total data variability and reveals strong to moderate positive loading on Sr, Fe, Cu, V, and Sc association. These elements (except for Sr) can be directly attributed to the metagabbroic rocks and igneous gabbroic rock due to their substitution in ferromagnesian minerals like, olivine, pyroxene, amphibole (Bhuiyan et al., 2011; Lapworth et al 2012; Papadopoulou- Vrynioti et al., 2013; Hao et al., 2014). Concerning Sr, it is possibly found in the crystal lattices of carbonate minerals (Šajn et al., 2013).

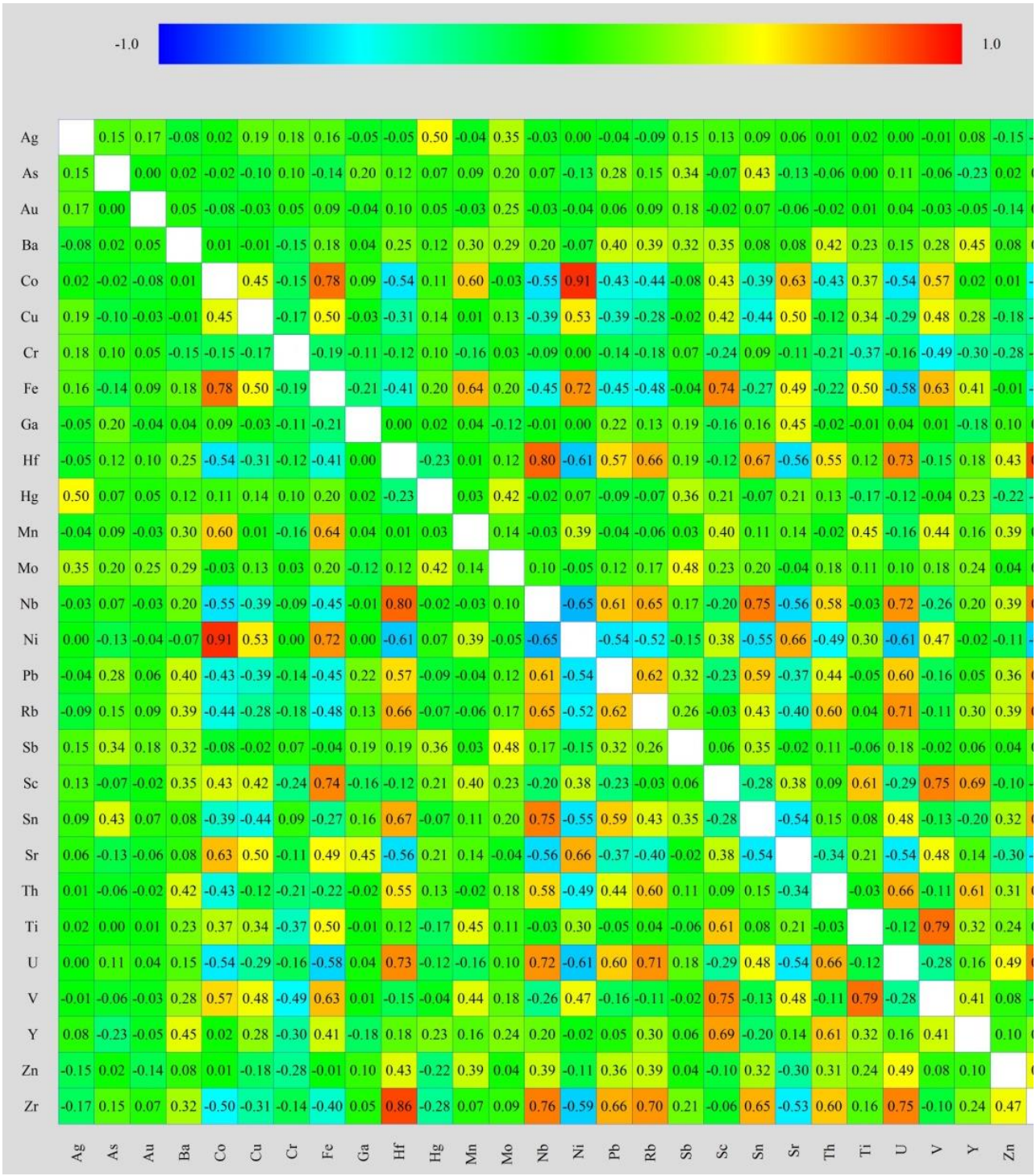

Table 4. Spearman–Rho correlation coefficient matrix of log_{10} transformed data of the chemical elements distributed in the studied rock sampling stations (N=105).

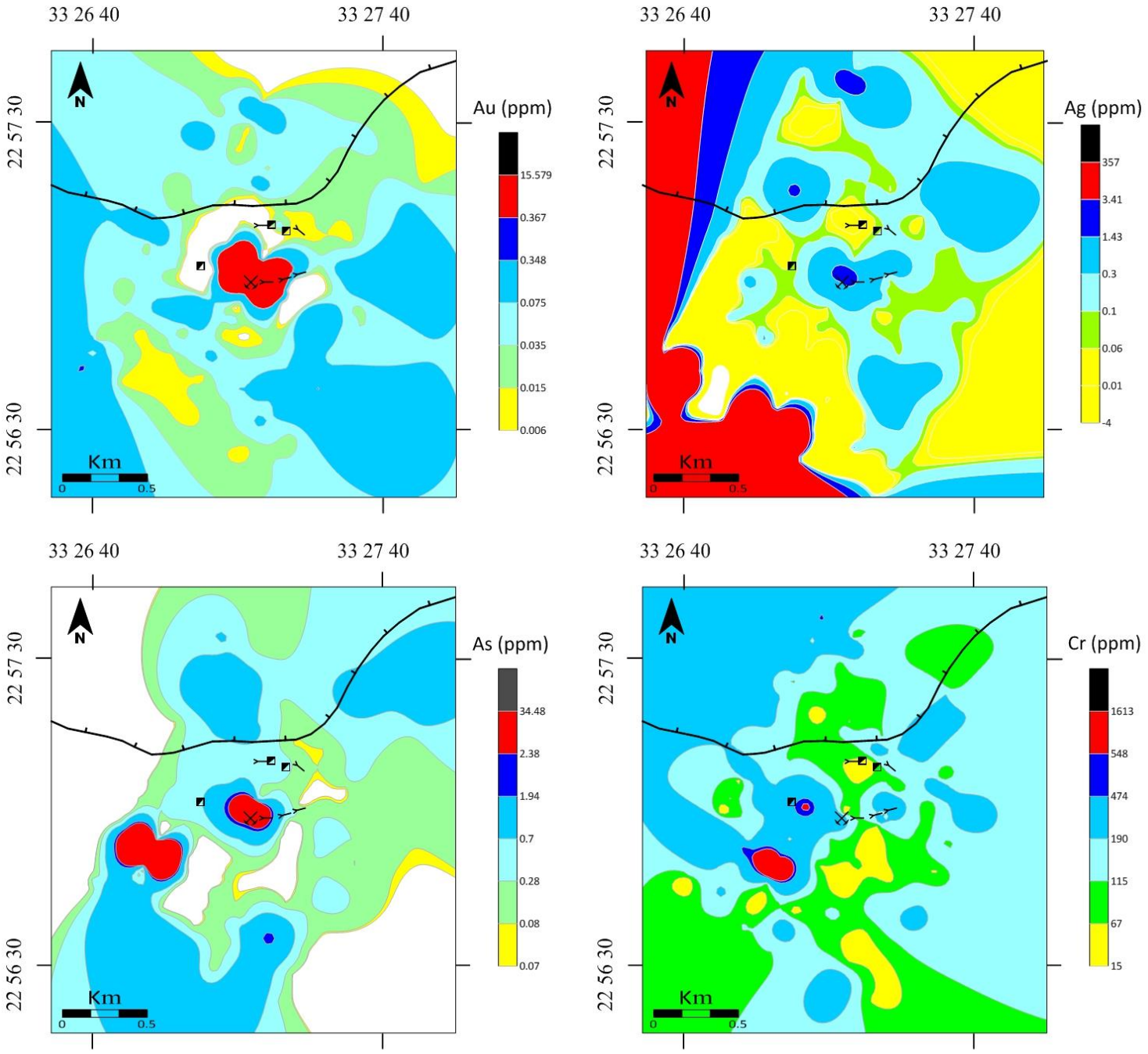

Fig.3. Geochemical maps for the spatial distributions of Au, Ag, As and Hg in the studied rock sampling stations (N=105).

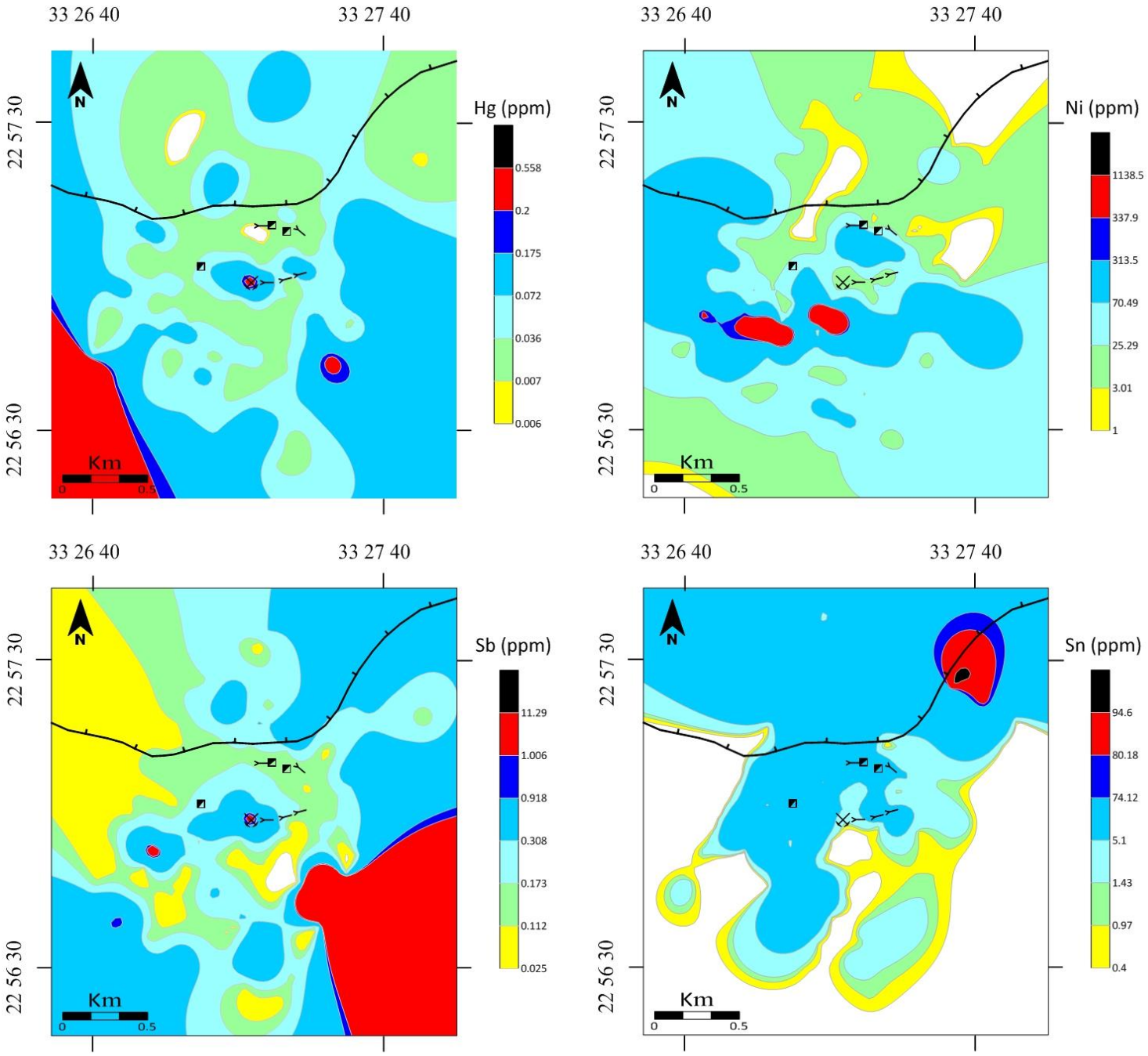

Fig.4. Geochemical maps for the spatial distributions of Sb, Cr, Ni and Sn in the studied rock sampling stations (N=105).

Concerning the mapping of the factor scores, the map of factor score F1 values (0.5-1.0) covers mainly the southern part of the mapped area and extends to the western part on both sides of the shear zone between the granite pluton and the metagabbroic rocks (Fig. 5). With the enhancement of factor score F1values (1.0-1.5), the spatial distribution patterns are mainly occurring at the south and southwest of the ancient Au-mine. The extreme higher values of factor score F1 (> 1.5) are commonly concentrated at the southwest of the Au mine. It can be seen that the primary

dispersion patterns of factor score F1 show a distinct relationship with the metagabbroic rocks so that it can be named "metagabbroic factor".

Factor 2 explains 8.19 of total data variability and illustrates moderate positive loading on Ti, Ni, and Fe association; it seems to be controlled by iron oxides and ferromagnesian minerals in dykes and mafic rocks.

Table 5. Results of communalities of factor analysis of $\log_{10}$ transformed data of the chemical elements distributed in the rock sampling stations (N=105).

Component	Initial Eigenvalues			Extraction Sums of Squared Loadings			Rotation Sums of Squared Loadings		
	Total	% of Variance	Cumulative %	Total	% of Variance	Cumulative %	Total	% of Variance	Cumulative %
1	4.730	16.891	16.891	4.730	16.891	16.891	2.875	10.268	10.268
2	3.003	10.725	27.616	3.003	10.725	27.616	2.292	8.185	18.453
3	2.304	8.228	35.844	2.304	8.228	35.844	2.232	7.970	26.423
4	1.606	5.735	41.580	1.606	5.735	41.580	2.197	7.847	34.271
5	1.483	5.296	46.876	1.483	5.296	46.876	2.090	7.464	41.735
6	1.385	4.948	51.823	1.385	4.948	51.823	1.761	6.289	48.024
7	1.223	4.368	56.192	1.223	4.368	56.192	1.483	5.297	53.321
8	1.178	4.206	60.398	1.178	4.206	60.398	1.480	5.285	58.606
9	1.110	3.965	64.363	1.110	3.965	64.363	1.357	4.845	63.451
10	1.049	3.747	68.110	1.049	3.747	68.110	1.304	4.658	68.110
11	.989	3.534	71.644						
12	.895	3.197	74.840						
13	.860	3.072	77.912						
14	.783	2.797	80.709						
15	.726	2.592	83.301						
16	.654	2.337	85.638						
17	.640	2.285	87.923						
18	.616	2.200	90.123						
19	.541	1.932	92.055						
20	.486	1.734	93.789						
21	.394	1.408	95.197						
22	.368	1.316	96.513						
23	.317	1.133	97.646						
24	.242	.865	98.511						
25	.146	.523	99.034						
26	.118	.422	99.455						
27	.092	.329	99.785						
28	.060	.215	100.000						

Extraction Method: principal component analysis, Rotation method: Varimax with Kaiser normalization.

At the same time, these elements are expected to be referred to disseminated Ni–sulfides and Ni–arsenides hosted by mafic rocks. This is proved by the high normalized mean value of Ni, which equals 5.49 and 1.46 in the metagabbroic unit and dykes, respectively. The geochemical map of factor score F2 reveals that the primary dispersion haloes of factor score F2 values (0.5-1.0) existed on both sides of the structure contact between the granitic and metagabbroic rocks (Fig. 5). In the same manner, the distribution haloes of factor score F2 values (1.0-1.5) and (> 1.5) form conspicuous separated patterns that are probably following the shear zones and hidden fracture system filled with the dykes. Therefore, factor score F2 can be termed "metagbbroic and dyke factor".

Factor 3 indicates 7.97 of total data variability and includes moderate positive loading on Th and Mo association and moderate negative loadings for Cr. This factor shows that the first two elements are likely involved in granitic rocks because Th is typically related to the felsic source and combined structurally in crystal lattices of zircon and monazite (Asami et al. 2002, Kitajima et al. 2012). Moreover, Mo might be accommodated in sulfide minerals associated with granitic rock. In contrast, the moderate negative loading for Cr is predictably confined to some silicate minerals and a few oxides because it is considered as common impurities in the structures of muscovite, biotite, chlorite, magnetite, and rutile.

The mapped high positive score F3 (ranging from 0.5 to 1.0) is predominantly distributed throughout the metagabbroic rocks (Fig. 5). Furthermore, the spatial distribution of the high and extremely high values of factor score F3 (1.0-1.5 and >1.5) appears mainly at the location of a deserted Au mine and its surrounding parts (the east, the south, and the southwest parts). This indicates that the granitoid pluton could play a significant role to feed the mineralized hydrothermal solutions to the structural zones in the metagabbroic rocks, and thus factor score F3 is dubbed "granitoid factor".

Factor 4 interprets 7.85 of total data variability, presents the association of strong to moderate positive loading on Ag, Sb, Au, and Hg.

Table 6 Results of rotated factor loadings of $\log_{10}$ transformed data of the chemical elements distributed in the rock sampling stations (N=105).

Element	Component				Communalities
	1	2	3	4	
Ag	-.084	.165	.198	**.817**	.741
As	-.048	.422	-.228	.188	.268
Au	-.011	-.057	.066	**.525**	.283
Ba	.084	.179	.463	.190	.289
Co	.259	.420	-.247	-.031	.305
Cr	.006	-.119	-.568	.255	.402
Cu	**.558**	.202	.146	-.041	.375
Fe	**.646**	**.540**	.228	.066	.766
Ga	.088	.166	.457	.045	.246
Hf	-.650	-.027	.157	-.007	.448
Hg	.401	-.244	.166	**.519**	.517
Mn	.148	**.780**	.240	-.031	.689
Mo	-.062	.158	**.557**	.165	.366
Nb	-.429	.037	.060	.085	.196
Ni	.482	**.664**	-.252	-.090	.744
Pb	-.016	-.053	.130	-.032	.021
Rb	-.348	.005	.410	.146	.311
Sb	-.098	.118	-.143	**.773**	.642
Sc	**.509**	.074	.273	.061	.343
Sn	-.051	-.372	-.224	-.125	.206
Sr	**.797**	.317	.110	.011	.749
Th	-.193	-.112	**.569**	-.394	.528
Ti	.087	**.665**	.490	-.160	.714
U	.012	-.035	.226	.156	.077
V	**.527**	.264	.391	-.081	.506
Y	.032	-.026	.341	.058	.122
Zn	-.485	.408	.287	-.255	.549
Zr	-.450	-.021	.174	-.070	.238

Extraction Method: principal component analysis, Rotation method: Varimax with Kaiser normalization, factor loading exceeding the absolute value of 0.5 are printed in bold.

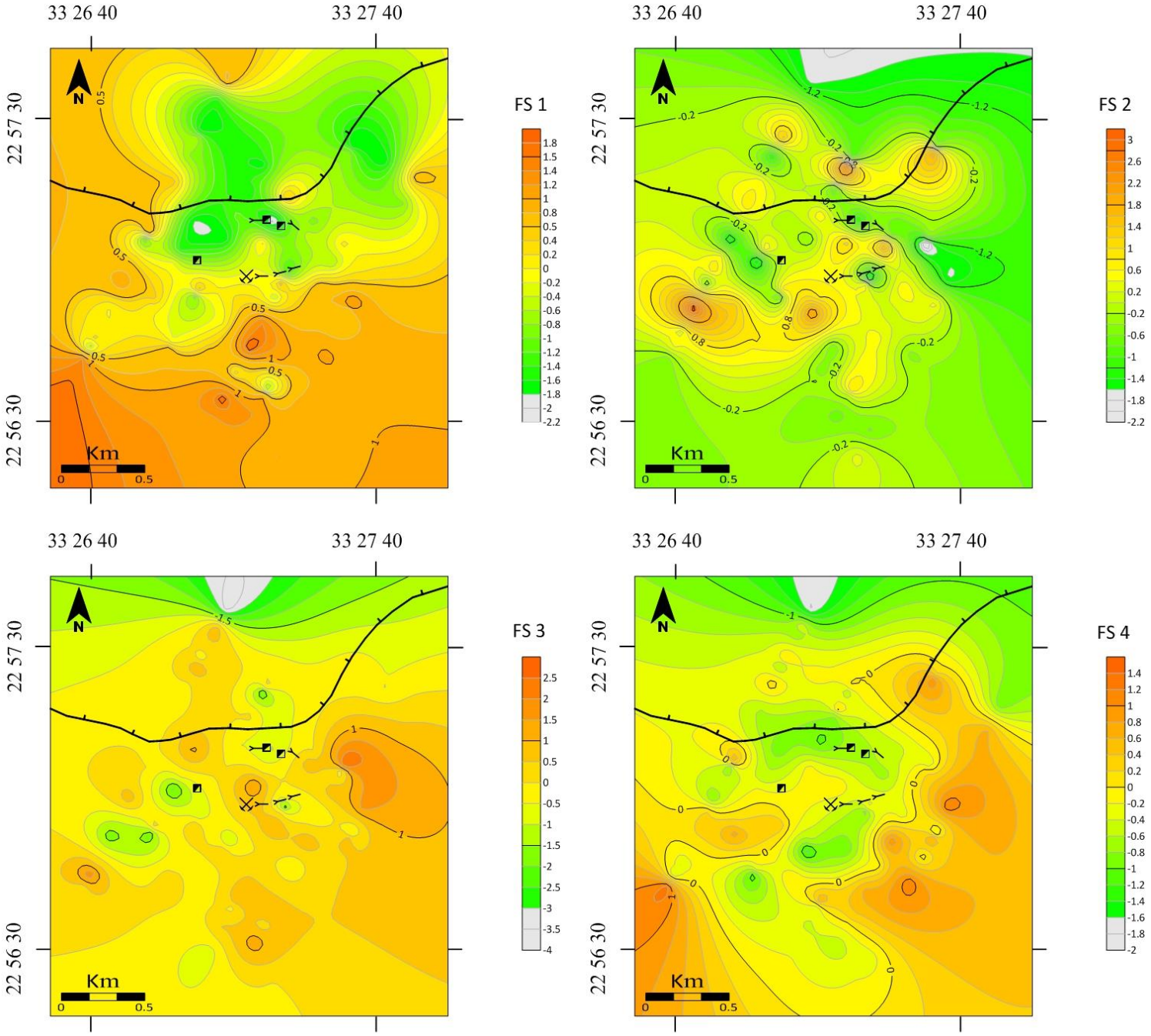

Fig.5. Geochemical maps for the spatial distributions of the four factor scores (FS1, FS2, FS3 and FS4) in the studied rock sampling stations (N=105).

It is named "Au- mineralization factor" because this association is closely related to the Au mineralization and the elements, such as Ag, Sb and Hg, are regarded as pathfinders for Au mineralization (Boyle and Jonasson, 1973; Boyle, 1979) and should be considered in all types of geochemical surveys (Reis et al., 2003, 2004). With respect to the spatial distribution map of factor score F4 (Fig. 5), the primary patterns of high positive scores (ranging from 0.5 to 1.0) are prevailing at the southeastern part and southwestern corner of the traversed area. It can be

concluded that the element association of factor 4 constituted Au- mineralization is derived from igneous hydrothermal solutions sourced by an emplacement of the granitoid pluton. Precisely for this reason, factor score F4 is considered as a guide of the presence of a new location of Au mineralization controlled by tectonic zones in plutonic mafic rocks at the Um Arka area. Undoubtedly, factor scores F4 association can give a clear image of new occurrences of Au mineralization which can be evaluated and exploited at present.

Cluster analysis

In order to obtain a complete image for a better understanding of the interrelation among the four-factor scores and emphasize their close association with geogenic sources, the hierarchical dendrogram generated by R-mode cluster analysis has been utilized. The produced dendrogram could group the four-factor scores generated by R-mode factor analysis into mathematically three clusters at a linkage distance of 10 (Fig. 6) as follows:

Cluster 1 consists of both factor scores F3 (granitoid factor) and factor score F4 (Au-mineralization factor) possessing a similar geochemical affinity. Therefore, it is regarded as a significant category and named "Au-mineralization and granite cluster". This cluster supports that Au mineralization is likely represented a separate mineralized event of the major episodes of mineralization in the area. For this reason, it gives an integrated image to emphasize that the geochemical signatures of mineralized hydrothermal solution forming Au-mineralization and related hydrothermal alteration zones have been sourced by the granitic intrusion in the study area.

Cluster 2 involves only factor score F1 (metagabbroic factor), possesses the lithologic nature, and is termed "metagabbroic cluster" too. Cluster 3 is separated and includes factor scores F2 alone (metagabbroic and dyke factor), and then it is called" metagabbroic and dyke cluster" too. At a linkage distance of 20, cluster 1 " Au-mineralization and granitoid cluster "can be merged with cluster 2 " metagabbroic cluster" to form the new category. In that case, the possible explanation is that Au bearing solution generated by the granitoid pluton could invade the structure zones in the metagabbroic rocks and precipitate Au- mineralization. Therefore, it can be proven that Au mineralization not only occurred in the form of quartz veins but also fills fracture system in the granitic and metagabbroic rocks.

Finally, at a linkage distance of 25, cluster 3 included factor scores F2 (metagabbroic and dyke factor) and possessed lithologic nature, could group with cluster 1 and cluster 2. In this case, it can be proved that the dykes in the study area are expected to be mineralized too.

Conclusions

The various techniques used for the treatment of geochemical data could achieve the goal of this study, presented a clear image and significant indications of the main aspect of the Au mineralization history, and provided important information on the economic evaluation of the Um Arka area. The present study detected significant new sites of Au mineralization hosted in the country rocks, dykes, and tectonic zones in addition to the quartz vein system. It confirmed that the abandoned Au mine is still fruitful and gives us much hope to start new mining operations of Au with expected success using the modern tools of technology at present. Besides Au-mineralization, new Sn- and Ni-mineralizations have probably occurred in the granitic and metagabbroic plutons, respectively.

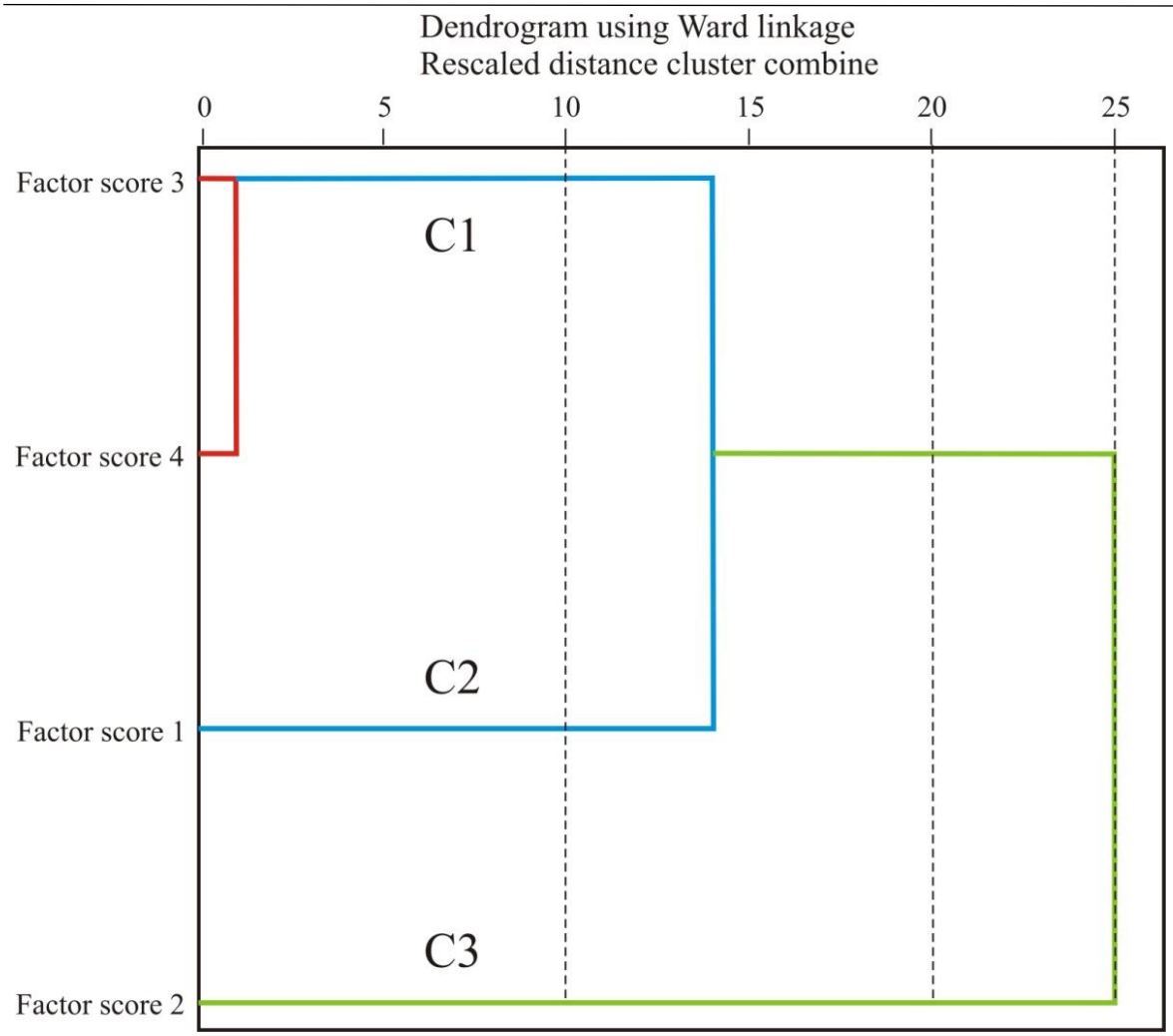

Fig. 6. Dendrogram of the hierarchical cluster analysis for four factor scores (FS1, FS2, FS3 and FS4) in the studied rock sampling stations (N=105).

Therefore, the aforementioned mineralizations are likely represented three independent mineralized events and constituted a predictable single major episode of mineralization sourced by hydrothermal solutions related to the granitoid pluton in the research area. Overall, spatial distributions of the stated mineralizations were predominantly controlled by lithology, tectonic zones, and supergene processes in this area. Undoubtedly, the Um Arka area is a fertile and promising location of Au mineralization, considered as a larger potential target area for Au, Ni, and Sn, and then it will give a prolific output for these elements in the future. All in all, the authors recommend carrying out geochemical exploration for hidden Au-mineralization using Ag, As, Hg, and Sb as pathfinder elements. Likewise, geochemical prospection of Ni - and Sn-mineralizations should be performed in the investigated area as well.

References

Abdel Rahman E.A., Qaaud N., Emam A. and Abdou N.M. (2013) Plutonites of Wadi Um Arka, Allaqi region, South Eastern Desert, Egypt: remote sensing and geochemical aspects. J.ournal of Biol. and Earth Sci. 3(2), 18-38.

Abdel Tawab M.M. (1992) Gold exploration in Egypt from Pharoanic to modern times, Zentralbl. Geol. Paläeontol. Teil 1, 2721–2733.

Asami M., Suzuki K. and Grew E.S. (2002) Chemical Th–U–total Pb dating by electron microprobe analysis of monazite, xenotime and zircon from the Archean Napier complex, East Antarctica: evidence for ultrahigh-temperature metamorphism at 2400 Ma. Precambr. Res. 114(3–4):249–275.

Bea F. (1996) Residence of REE, Y, Th and U in granites and crustal protoliths; implications for the chemistry of crustal melts. J. Petrol. 37, 521–552.

Beus A.A. and Grigorian S.V. (1977) Geo-chemical Exploration Methods for Mineral Deposits.Applied Pub. Co., Willmette Illinois, 278 pp.

Bhuiyan M.A.H., Rahman M.J.J., Dampare S.B. and Suzuki S. (2011) Provenance, tectonics and source weathering of modern fluvial sediments of the Brahmaputra–Jamuna River, Bangladesh: inference from geochemistry. J. Geochem. Explor. 111, 113–137.

Bouvier A.S., Ushikubo T., Kita N.T., Cavosie A.J., Kozdon R. and Valley J.W. (2012) Li isotopes and trace elements as a petrogenetic tracer in zircon: insights from Archean TTGs and sanukitoids. Contrib. Mineral. Petrol. 163, 745–768.

Boyle R.W. (1979) The geochemistry of gold and its deposits. Geol. Surv. . Canada, Bull. 280, 583.

Boyle R.W. and Jonasson I.R. (1973) The geochemistry of arsenic and its use as an indicator element in geochemical prospecting. J. Geochem. Explor. 2, 251–296.

Briggs P.L. (1978) Pattern Recognition Applied to Uranium Prospecting Submitted to the Department of Earth and Planetary Sciences, 233pp.

Broom-Fendley S., Brady A.E., Wall F., Gunn G. and Dawes W. (2016) REE minerals at the Songwe Hill carbonatite, Malawi: HREE enrichment in late-stage apatite. Ore Geol. Rev. https://doi.org/10.1016/j.oregeorev.2016.10.019.

Castillo-Munoz R. and Howarth R.J. (1976) Application of the empirical discriminant function to regional geochemical data from the United Kingdom. Geol. Soc. Am. Bull. 87,1567–1581.

Collyer P.L. and Merriam D.F. (1973) An application of cluster analysis inmineral exploration. Math. Geol. 4, 213–223.de Barros CE, Nardi LVS, Dillenburg SR, Ayup R, Jarvis K, Baitelli R (2010) Detrital minerals of modern beach sediments in southern Brazil: a provenance study based on the chemistry of zircon. J. Coast. Res. 26(1), 80–93.

Darwish M.A.G. (1996) Geochemical exploration in Um Qureiyat area, Wadi Allaqi, Southeastern Desert, Egypt, M.Sc. Thesis, South Valley Uni., Egypt.

Darwish M.A.G. (2004) Geochemical exploration for the gold in Haimur area, Wadi Allaqi, Southeastern Desert, Egypt, Ph.D. Thesis, South Valley Uni., Egypt.

EGSMA (1996) Geologic map of Wadi Jabjabah quadrangle, Egypt. Geol. Surv., Cairo, Egypt.

Eilu P. and Mikucki E.J. (1998) Alteration and primary geochemical dispersion associated with the Bulletin lode gold deposit, Wiluna, Western Australia. J. Geochem. Explor. 63, 73–103.

El Afandy A.H., El Mezayen A.M., Abdel Rahman E.M., Ammar, F.A. and Ahmed, A.A. (2007) Geological and geochemical studies of the Pan-African rocks at Wadi El Qulieb area, Southeastern Desert. Egypt. J. Fac. Sci. Minufia Uni. XXI, 159–195.

El-Alfy Z.S. (1986) Geological studies around Gebel Kulyiet, South Eastern Desert, Egypt, M.Sc. Thesis, Ain Shams Uni., Egypt.

El dosouky A.M., Abdelkareem M. and Elkhateeb S.O. (2017) Integration of remote sensing and aeromagnetic data for mapping structural features and hydrothermal alteration zones in Wadi Allaqi area, South Eastern Desert of Egypt. J. Afri. Earth Sci. 130, 28-37.

El-Desoky H.M. and El-Welaly M.R. (2018) Neoproterozoic ultramafic rocks from Wadi Umm Araka-Wadi Shakaib area, north Wadi Allaqi, south Eastern Desert, Dgypt: Insights into mineralogy and geochemistry of some mineral deposits. Annals Geol. Surv. Egypt. V. XXXV, 60 – 88.

El Fakhrany A.S.A. (1997) Geology of the area north Dineibit El-Quleib, Southeastern Desert, Egypt. Ph.D. Thesis. Faculty of Science ,Aswan University.

El Ramly M.F., Ivaanov S.S. and Kochin G.C. (1970) The occurrence of gold in the Eastern Desert of Egypt. Studies on some mineral deposits of Egypt. Part I, Section A, Metallic Minerals, Internal Report 021/1970, Geol. Surv. Egypt, 1–22 pp.

El Shimi K.M. (1996) Geology, structure and exploration of gold mineralization in Wadi Allaqi area SW, Eastern Desert Egypt, Ph.D. Thesis, Ain Shams Uni., Cairo, Egypt.

Fairbridge R.W. (1972) In: The encyclopedia of geochemistry and environmental science. Dowden, Hutchinson & Ross Inc., USA, IVA.

Fawzy S.M.A., Yousef M., Ghazaly M., El Amin H. and Abdel Hamid S. (2000) Metamorphic imprints of the area north of Denibit El Quleib, S.E.D., Egypt: evidence from metamorphic rocks for over thrusting. Annals Geol. Surv. Egypt. XXIII, 525–538.

Fawzy K.M., Abdel Rahman E.M. and Emam A.A. (2012) Mineralogical and geochemical studies on Haimur and Hariari gold deposits, Wadi Allaqi district, South Eastern Desert, Egypt. Ann. Geol. Sur. Egypt. V. XXXI (2009-2011), 319-348 pp.

Ferguson C. and Kasamas H. (1999) Risk assessment for contaminated sites in Europe. Policy framework, vol 2. LQM Press, Nottingham.

Fowler J., Cohen L. and Jarvis P. (1998) Practical Statistics for Field Biology. Chichester: John Wiley & Sons, 259 pp.

Fu B., Page F.Z., Cavosie A.J., Fournelle J., Kita N.T., Lackey J.S., Wilde S.A. and Valley J.W. (2008) Ti-in-zircon thermometry: applications and limitations. Contrib. Mineral. Petrol. 156, 197–215.

Govett G.J.S. and Atherden P.R. (1988) Applications of rock geochemistry to productive plutons and volcanic sequences. J. Geochem. Explor. 30, 223–242.

Guillén M.T., Delgado J., Albanese S., Nieto J.M., Lima A. and De Vivo B. (2011) Environmental geochemical mapping of Huelva municipality soils (SW Spain) as a tool to determine background and baseline values. J. Geochem. Explor. 109, 59–69.

Gustavsson N. and Bjorklund A. (1976) Lithological classification of tills by discriminant analysis. J. Geochem. Explor. 29, 89–103.

Hao L., Zhao X., Zhao Y., Lu J. and Sun L. (2014) Determination of the geochemical background and anomalies in areas with variable lithologies. J. Geochem. Explor. 139, 177–182.

Hoskin P.W.O. and Schaltegger U. (2003) The composition of zircon and igneous and metamorphic petrogenesis. In: Hanchar JM, Hoskin PWO (eds), Zircon. Rev. Mineral. Geochem, 53, 27–62.

Howarth R.J. (1973) The pattern recognition problem in applied geochemistry. In: Jones, M.J. (Ed.), Geochemical Exploration 1972. Institution of Mining and Metallurgy, London, 259–273.

Hume W.F. (1937) Geology of Egypt, vol. II, Part III. Geol. Surv. Egypt.

James C.H. (1967) The use of the terms "primary" and "secondary" dispersion in geochemical prospecting. Econ. Geol. 62, 997-999.

Jiao S., Guo J., Harley S.L. and Peng P. (2013) Geochronology and trace element geochemistry of zircon, monaziteand garnet from the garnetite and/or associated other high-graderocks: implications for Palaeoproterozoic tectonothermal evolution ofthe Khondalite Belt, North China Craton. Precambr. Res. 237,78–100.

Jordan C., Zhang C. and Higgins A. (2007) Using GIS and statistics to study influences of geology on probability features of surface soil geochemistry in Northern Ireland. J. Geochem. Explor. 93,135–152.

Kaiser H.F. (1958) The varimax criterion for analytic rotation in factor analysis. Psychometrika 23, 187–200.

Khalil F A, ElmAnawy M.E.O., Hasssan A.A., Ghieth B.M. and Aref A.A.F. (2003) Application of some geophysical techniques on aeromagnetic data to delineate the tectonic structuresof Wadi Heisurba area, south Eastern Desert, Egypt. 3rd Intern. Conf. on Geol. of Africa, 1, 447-490.

Khalil A.E., Obeid M.A. and Azer M.K. (2014) Serpentinized peridotites at the north part of the Wadi Allaqi district (Egypt): Implications for the tectono-magmatic evolution of Fore-Arc Crust. Acta Geologica Sinica (English Edition), 88(5), 1421-1436.

Kitajima K., Ushikubo T., Kita N.T., Maruyama S. and Valley J.W. (2012) Relative retention of trace element and oxygen isotope ratios in zircon from Archean rhyolite, Panorama Formation, North Pole Dome, Pilbara Craton,Western Australia. Chem. Geol. 332–333, 102–115.

Klemm R. and Klemm D. (2013) Gold and gold mining in ancient Egypt and Nubia. Springer, Berlin, 649 pp.

Kochin G.G. and Bassyouni F.A. (1968) Mineral resource of the UAR. (Part I Metallic minerals) Geological Survey Egypt, Internal Report 1968/013, 493 pp.

Lapworth D.J., Knights K.V., Key R.M., Johnson C.C., Ayoade E., Adekanmi M.A., Arisekola T.M., Okunlola O.A., Backman B., Eklund M., Everett P.A., Lister R.T., Ridgway J., Watts M.J., Kemp S.J. and Pitfield P.E.J. (2012) Geochemical mapping using stream sediments in west-central Nigeria: implications for environmental studies and mineral exploration in West Africa. Appl. Geochem. 27, 1035–1052.

Lin X., Wang X., Zhang B. and Yao W. (2014) Multivariate analysis of regolith sediment geochemical data from the Jinwozi gold field, north-western China. J. Geochem. Explor. 137, 48–54.

Martínez J., Llamas J., de Miguel E., Rey J. and Hidalgo M.C. (2007) Determination of the geochemical background in a metal mining site: example of the mining district of Linares (South Spain). J. Geochem. Explor. 94, 19-29.

Maynard J.B. (1983) *Geochemistry of sedimentary ore deposits*. Springer-Verlag, New York, 305 pp.

McCuaig T.C. and Kerrich R. (1998) P–T–t-deformation-fluid characteristics of lode gold deposits: evidence from alteration systematics. Ore Geol. Rev. 12, 381–453.

Meneisy M.Y., El-Kalyouby B.A. and Alfy Z.S. (1986) Petrogenesis and geochronology of the granitic intrusions of Gebel Kulyiet and Seiga, south Eastern Desert, Egypt, Qatar, Univ. Sci. Bull. 6, 287–315.

Noweir A.M., El-Amawy M.A., Rashwan A.A. and Abdel-Aziz A.M. (1996) Geology and structural evolution of the pan-african basement rocks around Wadi Umm Araka, Northeast Wadi Allaqi, South Eastern Desert, Egypt. Egypt J. Geol. 40 (2), 477-512.

Noweir A.M, Rashwan A.A., Abu El Ela A.M. and El Hashash M.A.A. (2001) Petrology, petrochemistry and crustal evolution of the Precambrian rocks, Wadi Um Ashira, South Eastern Desert, Egypt. Annals of the Geological Survey of Egypt, Annals of the Geological Survey of Egypt Cairo,V. XXIII (3), 961-981.

Noweir A.M., Rashwan A.A. and Mehanna A.M. (2007) Genesis of the maficultramafic and related metamorphic rocks in the Northwestern part of Wadi Allaqi Terrain-South Eastern Desert, Egypt. Ann. Geol. Surv. Egypt, 29, 51-75.

Ohta A., Imai N., Terashima S. and Tachibana Y. (2005) Application of multielement statistical analysis for regional geochemical mapping in Central Japan. Appl. Geochem. 20, 1017–1037.

Ohta A., Imai N., Terashima S., Tachibana Y., Ikehara K., Okai T., Ujiie-Mikoshiba M. and Kubota R. (2007) Elemental distribution of coastal sea and stream sediments in the island-arc region of Japan and mass transfer processes from terrestrial to marine environments. Appl. Geochem. 22, 2872–2891.

Pantazis T.M. (1988) Lithogeochemical prospecting. In: General Geology. Encyclopedia of Earth Science. Springer, Boston, MA.

Papadopoulou-Vrynioti K., Alexakis D., Bathrellos G.D., Skilodimou H.D., Vryniotis D., Vassiliades E. and Gamvroula D. (2013) Distribution of trace elements in stream sediments of Arta plain (western Hellas): the influence of geomorphological parameters. J. Geochem. Explor. 134, 17–26.

Pirajno, F., Bagas, L., 2008. A review of Australia's Proterozoic mineral systems and genetic models. Precambr. Res. 166, 54–80.

Pohl W. (1988) Precambrian metallogeny of NE-Africa, in: S. El Gaby and R.O. Greiling (Eds.), The Pan-African Belt of NE Africa and Adjacent Areas, Friedrich Vieweg & Sohn Verlagsgesellschaft mbH, Braunschweig/Wiesbaden, Germany, 319–341 pp.

Reedman J.H. (1979) Techniques in mineral exploration. Applied Science Publishers, London, 534 pp.

Reimann C. and Filzmoser P. (2000) Normal and lognormal data distribution in geochemistry: death of a myth. Consequences for the statistical treatment of geochemical and environmental data. Environ. Geol. 39,1001–1014.

Reis A.P., Sousa A.J. and Fonseca E.C. (2003) Application of geostatistical methods in gold geochemical anomalies identification (Montemor-O-Novo, Portugal). J. Geochem. Explor. 77, 45–63.

Reis A.P., Sousa A.J., Ferreira da Silva E., Patinha C. and Fonseca E.C. (2004) Combining multiple correspondence analyses with factorial kriging analysis for geochemical mapping of the gold–silver deposit at Marrancos (Portugal). Appl. Geochem. 19, 623–631.

Sabet A.H. and Bordonosov V.P. (1984) The gold ore formations in the eastern Desert of Egypt, Ann. Geol. Surv. Egypt 16, 35–42.

Safronov N.I. (1936) Dispersion haloes of ore deposits and their use in exploration. Problemy Sovetskoy Geologii 4, 41–53.

Šajn R., Aliu M., Stafilov T. and Alijagić J. (2013) Heavy metal contamination of topsoil around a lead and zinc smelter in Kosovska Mitrovica/Mitrovicë, Kosovo/Kosovë. J. Geochem. Explor. 134, 1–16.

Stein M. and Goldstein S.L. (1996) From plume head to continental lithosphere in the Arabian-Nubian Shield. Nature 382, 773–778.

Stern R.J. (1994) Arc assembly and continental collision in the Neoproterozoic East African Orogen: implications for the consolidation of Gondwanaland. Ann. Rev. Earth. Planet. Sci. 22, 319–351.

Tayae A.A. (2005) Mineralogical and geochemical studies on some gold deposits and host rocks, Wadi Allaqi, South Eastern Desert, Egypt, Ph.D. Thesis, South Valley Uni., Egypt.

Taylor S.S. and Mclennan M.S. (1995) The geochemical evolution of the continental crust. Rev. Geophys. 33 (2), 241–265.

Tukey J.W. (1997) Exploratory data analysis. Addison-Wesley Publishing 7 Company, Massachusett.

van Helvoort P.J., Filzmoser P. and van Gaans P.F.M. (2005) Sequential factor analysis as a new approach to multivariate analysis of heterogeneous geochemical datasets: an application to a bulk chemical characterization of fluvial deposits (Rhine–Meuse delta, The Netherlands). Appl. Geochem. 20, 2233–2251.

Varajão C.A.C., Colin F., Vieillard P., Melfi A.J and Nahon D. (2000) Early weathering of palladium gold under lateritic conditions, MaquineÂ Mine, Minas Gerais, Brazil, Appl. Geochem. 15, 245–263.

Wilde A.R., Bierlein F.P. and Pawlitschek M. (2004) Lithogeochemistry of orogenic gold deposits in Victoria, SE Australia: a preliminary assessment for undercover exploration. J. Geochem. Explor. 84, 35–50.

Williams T.M., Dunkley P.N., Cruz E., Acitimbay V., Gaibor A., Lopez E., Baez N. and Aspden J.A. (2000) Regional geochemical reconnaissance of the Cordillera Occidental of Ecuador: economic and environmental applications. Appl. Geochem. 15, 531–550.

Xie X., Liu D., Xiang Y., Yan G. and Lian C. (2004) Geochemical blocks for predicting large ore deposits-concept and methodology. J. Geochem. Explor. 84, 77–91.

Xuejing X. and Binchuan Y. (1993) Geochemical pattern from local to global. J. Geochem. Explor. 47, 109–129.

Zhang C., Manheim F.T., Hinde J. and Grossman J.N. (2005) Statistical characterization of a large geochemical database and effect of sample size. Appl. Geochem. 20, 1857–1874.